buildings

MDPI

Article

Research on the Evaluation of Prefabricated MEP Systems for Energy Stations Based on the AHP–Entropy–Fuzzy Model

Yuxuan Liu [1], Fan Zhang [2], Shuqiang Gui [3,*], YungHao Loh [1], Myzatul Aishah Kamarazaly [1,*] and Jiaji Zhang [4,5,6,*]

[1] School of Architecture, Building and Design, Taylor's University, Subang Jaya 47500, Selangor, Malaysia; 0379486@sd.taylors.edu.my (Y.L.); 0376795@sd.taylors.edu.my (Y.L.)
[2] Wuhan Hengtai Hongan Safety Technology Co., Ltd., Wuhan 430070, China; fanzhang_lab@163.com
[3] School of Urban Construction, Anhui Xinhua University, Hefei 230088, China
[4] Sanya Science and Education Innovation Park, Wuhan University of Technology, Sanya 572025, China
[5] School of Civil Engineering and Architecture, Wuhan University of Technology, Wuhan 430070, China
[6] Birmingham Centre for Energy Storage & School of Chemical Engineering, University of Birmingham, Birmingham B152TT, UK
* Correspondence: 003117@wsgri.com (S.G.); myzatulaishah.kamarazaly@taylors.edu.my (M.A.K.); zhangjiaji@whut.edu.cn (J.Z.)

Abstract

Prefabricated mechanical, electrical, and plumbing (MEP) systems have been increasingly adopted in energy station projects; however, systematic evaluation frameworks capable of integrating construction performance, cost constraints, and uncertain multi-indicator assessments remain limited. To address this gap, this study constructs an Analytic Hierarchy Process (AHP)–Entropy–Fuzzy evaluation framework to assess the comprehensive benefits of BIM-enabled prefabricated MEP construction in energy stations. A hierarchical evaluation system was established based on five dimensions: schedule, quality, cost, safety, and environmental performance, and ten secondary indicators were defined. The Analytic Hierarchy Process was used to determine expert-based subjective weights, the entropy method was applied to capture objective data variability, and multiplicative normalization was employed to obtain combined weights. A fuzzy comprehensive evaluation model was then introduced to transform heterogeneous construction records into comparable benefit levels and scores. The prefabricated method scored 87.80 and was classified as "high", whereas the conventional method scored 60.85 and was classified as "low". A Technique for Order Preference by Similarity to Ideal Solution (TOPSIS)-based sensitivity analysis further showed that, under 10%, 20%, and 50% criterion-weight perturbations, the prefabricated group consistently achieved higher closeness coefficients than the conventional group. The smallest margin occurred when the schedule weight was reduced by 50%, but the prefabricated group retained a positive advantage. The results demonstrate that Building Information Modeling (BIM)-enabled prefabricated MEP construction can achieve superior overall project performance through the coordinated optimization of schedule, cost, safety, quality, and environmental objectives, offering a practical evaluation framework and decision-support tool for the industrialized delivery of future energy infrastructure projects.

Keywords: prefabricated MEP systems; energy station; BIM; AHP–entropy method; fuzzy comprehensive evaluation; construction performance evaluation

Check for updates

Academic Editor: Ahmed Senouci

Received: 20 May 2026
Revised: 11 June 2026
Accepted: 15 June 2026
Published: 23 June 2026

Copyright: © 2026 by the authors. Licensee MDPI, Basel, Switzerland. This article is an open access article distributed under the terms and conditions of the Creative Commons Attribution (CC BY) license.

1. Introduction

1.1. Research Background

With the rapid advancement of urbanization and the global pursuit of carbon neutrality, the transformation of building energy systems toward low-carbon, efficient, and intelligent configurations has become a critical research focus [1]. In this context, district heating and cooling systems have attracted increasing attention because they can integrate centralized energy conversion, distribution, and demand-side management at the urban scale. These systems provide technical, economic, and environmental potential for improving urban energy efficiency and supporting the low-carbon transition [2,3]. As key infrastructure nodes in district heating and cooling networks, energy stations undertake centralized heating and cooling production and play an important role in improving energy utilization efficiency and reducing greenhouse gas emissions [4]. Consequently, urban district energy station projects have experienced rapid growth in recent years, particularly in China [5].

Against this backdrop, prefabricated construction technologies, characterized by reduced construction time, improved quality control, and enhanced sustainability, have gradually emerged as a key approach for promoting the industrialization of the construction sector [6]. Industrialized construction also indicates that digital technologies and factory-based production can improve standardization, productivity, and construction process integration, although their application depth varies across building systems and project types [7]. Many scholars have carried out extensive research on prefabricated electromechanical technologies for energy stations, covering various aspects such as system design, component prefabrication, on-site installation, and performance testing, which has promoted the initial application of this technology in engineering practice. Zhang et al. [8] introduced the prominent advantages of applying BIM technology in prefabricated projects for complex energy station equipment rooms and explored the implementation pathways. Zhang et al. [9] explored the typical applications of modular prefabricated assembly construction in building mechanical and electrical engineering, as well as methods for coordinated construction with building prefabrication, demonstrating the development trend of prefabricated mechanical, electrical, and plumbing (MEP) systems. GUO et al. [10] developed an intelligent control framework for optimizing the internal spatial arrangement of energy stations. It can be found that current prefabricated MEP projects for energy stations mainly suffer from problems such as insufficient construction coordination, inaccurate installation precision, and rising construction costs. Lavikka et al. [11] discussed value creation in MEP prefabrication from the standpoint of systemic innovation implementation. Valkonen et al. [12] further focused on tolerance management in prefabricated MEP installation.

Prefabricated construction demonstrates significant sustainability advantages throughout its life cycle, primarily in terms of reducing material waste, improving resource utilization efficiency, lowering carbon emissions, and enhancing environmental friendliness. In recent years, studies have further examined the environmental benefits of prefabricated systems from the perspectives of life cycle assessment and low-carbon construction. Cheng et al. [13] argued that prefabricated construction can significantly reduce on-site construction waste generation through industrialized production methods, while improving overall resource utilization efficiency, thereby enhancing the environmental performance of construction projects. Gallo et al. [14] reported that prefabricated construction exhibits synergistic advantages in energy consumption control and construction efficiency improvement, thereby supporting the transition of the construction industry toward lower energy use and higher efficiency. Ding et al. [15] concluded that BIM-based prefabricated construction methods have been proven to enhance sustainable project delivery by en-

abling life-cycle information integration and multi-stakeholder coordination optimization, thereby achieving improved resource allocation and low-carbon construction management. Compared with precast concrete prefabrication, the promotion of prefabricated MEP technologies has lagged significantly [16]. The root cause of this problem is that the academic community currently lacks a systematic and comprehensive evaluation framework for prefabricated MEP systems, particularly one capable of effectively integrating both qualitative and quantitative indicators.

In terms of evaluation methodology research, many scholars have carried out extensive exploratory work on precast concrete prefabrication systems. Zhai et al. [17] developed a Design for Assembly (DFA) evaluation method for prefabricated buildings, which combines formula design, the Delphi method, and the Analytic Hierarchy Process (AHP), providing an important theoretical research foundation for evaluating and improving the construction efficiency of prefabricated buildings. Similarly, Liu et al. [18] applied an AHP–Entropy combined weighting approach to evaluate the performance of prefabricated component suppliers, demonstrating the integration of subjective expert judgment with objective data-driven measures. Xia et al. [19] proposed a comprehensive risk assessment framework for prefabricated construction under the Engineering, Procurement, and Construction (EPC) model model, highlighting the need for systematic and quantitative evaluation methods. Solapure et al. [20] presented a comprehensive evaluation framework integrating the AHP–Entropy method to assess economic sustainability in precast and cast-in situ construction. Collectively, these studies indicate that AHP and entropy methods have become increasingly important in multi-criteria decision-making for prefabricated systems. At the broader construction level, multi-criteria decision-making (MCDM) methods have also been widely reviewed as effective tools for handling complex construction decision problems involving multiple and sometimes conflicting criteria [21]. In addition, recent reviews on BIM–MCDM integration show that existing applications mainly concentrate on sustainability, retrofit, supplier selection, safety, and constructability, whereas the application of integrated MCDM frameworks to BIM-enabled prefabricated MEP systems in energy stations remains underexplored [22].

Despite these advancements, prefabricated MEP systems in energy stations still lack a comprehensive evaluation framework that can simultaneously capture structural integration, operational efficiency, installation accuracy, cost-effectiveness, and sustainability. Most existing studies focus on discrete technical aspects such as module division, tolerance control, or BIM-enabled collaboration, but few provide a holistic assessment across multiple dimensions and criteria [23,24]. Moreover, although BIM has been widely recognized as a key information-support technology for off-site manufacturing, prior studies have focused more on conventional construction than on off-site manufacturing, and the specific evaluation of BIM-enabled prefabricated MEP systems in complex energy station plant rooms remains insufficient [25]. This gap limits the ability of engineers and project managers to make informed decisions regarding design optimization, technology selection, and performance trade-offs.

To address this challenge, multi-criteria decision-making (MCDM) approaches, particularly those integrating AHP, entropy weighting, and fuzzy comprehensive evaluation, offer a promising solution [26]. In the context of prefabricated MEP systems for energy stations, the evaluation problem involves both quantitative construction records and qualitative management-related indicators, while significant uncertainty and trade-offs exist among schedule, cost, safety, and environmental objectives. Using a single evaluation method is therefore insufficient to fully capture the complexity of the decision-making process. Specifically, AHP is effective in incorporating expert knowledge and engineering priorities, but it is inherently subjective and may introduce bias in weight determination.

In contrast, the entropy method can objectively reflect the variability and discriminative power of indicator data, yet it lacks the capability to represent managerial preferences and practical engineering experience. Furthermore, many evaluation indicators in prefabricated MEP construction exhibit fuzzy boundaries and linguistic uncertainty, which cannot be adequately addressed through deterministic weighting approaches alone. Therefore, the integration of AHP, entropy weighting, and fuzzy comprehensive evaluation enables the proposed framework to simultaneously balance expert cognition, objective data characteristics, and uncertainty handling, thereby providing a more reliable and comprehensive evaluation approach for complex energy station projects [27].

In this study, a comprehensive evaluation framework for prefabricated MEP systems in energy stations is developed based on the AHP–Entropy–Fuzzy model. The research focuses on four main aspects as follows:

(1) A multi-dimensional evaluation index system is established by considering key factors such as construction progress, quality, cost, and environmental performance, thereby forming a structured and hierarchical evaluation framework.
(2) A combined weighting approach is proposed, in which subjective weights derived from the AHP are integrated with objective weights obtained from the entropy method, enhancing the scientific robustness and reliability of the evaluation results.
(3) A fuzzy comprehensive evaluation method is employed to construct membership functions and evaluation matrices, enabling the calculation of overall performance scores.
(4) The proposed framework is further validated through a practical engineering case, demonstrating its applicability and effectiveness in assessing prefabricated energy station systems.

1.2. Research Framework

Based on the identified research gaps, this study establishes a framework that integrates the research logic, core content, and methodological procedures for evaluating prefabricated MEP systems in energy stations, as shown in Figure 1. First, through a comprehensive literature review, the research background is clarified, and key deficiencies in existing studies, particularly the lack of systematic and comprehensive evaluation frameworks are identified, leading to the formulation of an overall research framework. Second, a multi-dimensional evaluation system is constructed, incorporating five key dimensions: progress, quality, cost, safety, and environmental performance. Within this framework, ten secondary indicators are defined and categorized into state-based and comparative indicators. A combined weighting model is then developed by integrating the Analytic Hierarchy Process (AHP) with the entropy method, enabling the coupling of subjective judgment and objective data for more reliable weighting. Finally, a fuzzy comprehensive evaluation approach is adopted to establish the evaluation set, membership functions, and fuzzy relation matrix, through which the comprehensive evaluation vector and overall performance score are obtained. The proposed methodology is further validated through a case study, including a comparative analysis of construction benefits, thereby demonstrating the effectiveness and applicability of the technical route.

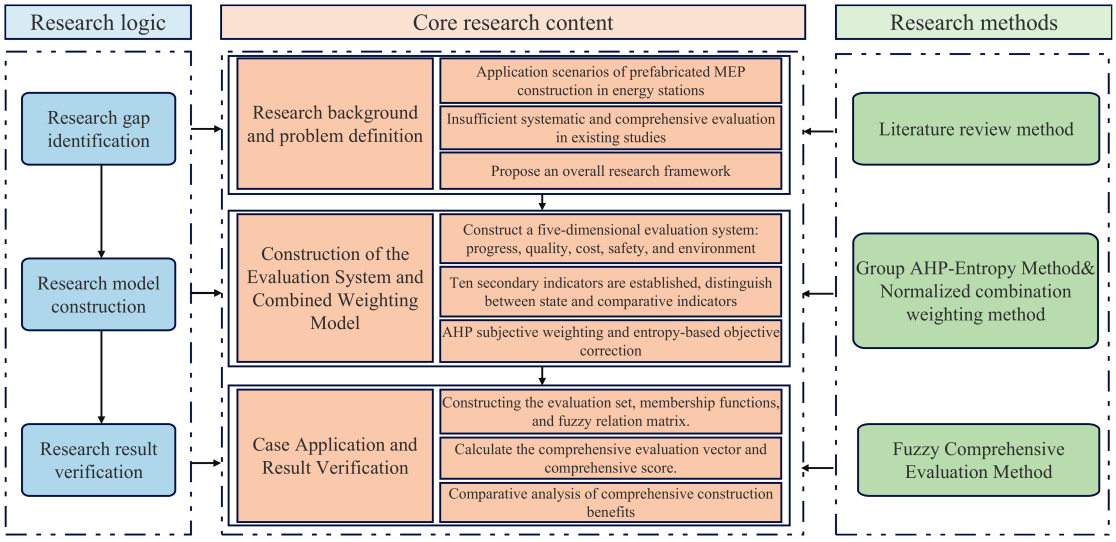


Figure 1. Research framework in this study.

2. Models and Methods

2.1. AHP–Entropy Model Construction

The AHP–Entropy model is a hybrid weighting approach that integrates subjective judgment with objective data characteristics and is widely applied in multi-criteria decision-making problems. This model employs the AHP to capture decision-makers' experiential knowledge by constructing pairwise comparison matrices to derive subjective weights of indicators [28]. Meanwhile, the entropy method measures indicator dispersion based on the information entropy of sample data, thereby determining objective weights [29]. The integration of these two methods effectively overcomes the limitations of using a single weighting approach: AHP prevents the neglect of practical importance inherent in purely data-driven methods, while the entropy method reduces the bias introduced by subjective judgment, thus enhancing the scientific rigor and reliability of weight determination [30]. This hybrid weighting strategy is consistent with the data structure of this study, where expert judgment is required to reflect engineering management priorities, while construction ledger data are used to capture the objective variability of different indicators.

Specifically, in the AHP method, a pairwise comparison matrix $\mathbf{A} = (a_{ij})$ is constructed, and the normalized eigenvector corresponding to the maximum eigenvalue is calculated to obtain the subjective weights w_i^{AHP}. A consistency check (Consistency Ratio, CR) is then performed to ensure the reliability of the judgment matrix.

In the entropy method, the original data are first normalized to obtain the matrix p_{ij}, and the information entropy of the j indicator is calculated as Formula (1).

$$e_j = -k\sum_{i=1}^{n} p_{ij}\mathrm{In}p_{ij},\ k = \frac{1}{\mathrm{In}n} \tag{1}$$

Based on this, the degree of divergence is computed as $d_j = 1 - e_j$, and the objective weight is determined by Formula (2).

$$w_j^{Entropy} = \frac{d_j}{\sum d_j} \tag{2}$$

2.2. Evaluation Index System Construction

To construct the evaluation index system, this study focuses on the practical engineering characteristics of prefabricated MEP systems in energy stations and establishes a

hierarchical evaluation framework. The overall objective layer is defined as the Comprehensive benefit (G), while the criterion layer is structured into five dimensions: Schedule benefit (C_1), Quality benefit (C_2), Cost benefit (C_3), Safety benefit (C_4), and Environmental benefit (C_5). Based on this structure, a multi-level evaluation index system is developed. The index system was derived from literature-informed screening and expert consultation, with project ledger availability used as a practical validation criterion [24,31]. It comprises five domains aligned with core construction management objectives. The ten secondary indicators were retained only when supported by auditable acceptance, commissioning, cost, safety, dust-monitoring, or waste records.

Specifically, ten secondary indicators are defined. For schedule benefit, I_{11} (Schedule improvement rate) is introduced. For quality benefit, three indicators are considered: I_{21} (First-time acceptance pass rate), I_{22} (First-pass commissioning success rate), and I_{23} (Reduction rate of rework input). For cost benefit, I_{31} (Total cost variation rate) is employed. For safety benefit, three indicators are defined: I_{41} (Reduction rate of high-risk operation exposure index), I_{42} (Reduction rate of near-miss incident frequency), and I_{43} (Timely closure rate of safety hazards). For environmental benefit, I_{51} (Reduction rate of construction waste) and I_{52} (Dust compliance rate) are included. The comprehensive benefit evaluation index system for prefabricated MEP systems in energy stations is shown in Table 1.

Table 1. Comprehensive benefit evaluation index system for prefabricated MEP systems in energy stations.

Objective Layer	Criterion Layer	Indicator Layer
Comprehensive benefit (G)	Schedule benefit (C_1)	I_{11} Schedule improvement rate
	Quality benefit (C_2)	I_{21} First-time acceptance pass rate I_{22} First-pass commissioning success rate I_{23} Reduction rate of rework input
	Cost benefit (C_3)	I_{31} Total cost variation rate
	Safety benefit (C_4)	I_{41} Reduction rate of high-risk operation exposure index I_{42} Reduction rate of near-miss incident frequency I_{43} Timely closure rate of safety hazards
	Environmental benefit (C_5)	I_{51} Reduction rate of construction waste I_{52} Dust compliance rate

(1) Schedule Benefit

The schedule improvement rate (I_{11}) is used to quantify the degree of compression in the critical path duration achieved by prefabricated MEP construction in energy stations compared with conventional construction methods.

(2) Quality Benefit

The first-time acceptance pass rate (I_{21}) is used to measure the proportion of MEP installation outcomes that meet acceptance standards during the initial inspection, reflecting the effectiveness of standardized manufacturing and BIM-enabled coordination in controlling installation deviations and errors such as omissions and clashes.

The first-pass commissioning success rate (I_{22}) is used to evaluate the ability of a system to achieve performance compliance during the initial commissioning stage and serves as a key indicator of system integration quality. Compared with evaluations based solely on installation acceptance, the commissioning process is more effective in revealing potential issues related to interface compatibility, control logic, and system coordination.

The reduction rate of rework input (I_{23}) is used to characterize the decrease in the proportion of rework labor hours required to correct quality deviations relative to a baseline. Compared with the single indicator of first-pass acceptance rate, this metric more effectively captures the process-related losses caused by hidden rework and repeated installation prior to formal acceptance and reflects the true cost of quality deviations from the perspective of resource consumption.

(3) Cost Benefit

The total cost variation rate (I_{31}) measures the direct construction stage cost difference between prefabricated MEP construction and conventional installation. It does not include life-cycle operation, maintenance, downtime, or carbon-related costs.

(4) Safety Benefit

The reduction rate of the high-risk operation exposure index (I_{41}) is used to evaluate the extent to which high-risk operations are reduced at the source. Compared with conventional construction methods in energy stations, which frequently involve cutting, grinding, and hot work operations, prefabricated construction reduces on-site processing through factory-based production. Combined with BIM-enabled safety rule checking and design-stage risk assessment, this approach effectively decreases both the intensity and frequency of high-risk operation exposure.

The reduction rate of near-miss incident frequency (I_{42}) is used to characterize the decrease in the frequency of near-miss events relative to a baseline. Compared with accident rates, which are highly sensitive to sample size, near-miss incidents serve as leading safety indicators that more reliably reflect risk exposure levels. In this study, the frequency of near-miss events is normalized by working hours and further converted into a reduction rate to ensure consistency in indicator direction.

The timely closure rate of safety hazards (I_{43}) measures the proportion of hazards that are resolved within a specified time frame, reflecting the efficiency of risk management. Prefabricated construction of energy station MEP systems improves hazard controllability by reducing complex on-site operations. Meanwhile, BIM-supported technologies, including risk information integration, visual positioning, and dynamic monitoring, optimize hazard identification and management processes, thereby shortening the remediation cycle and enhancing closure timeliness.

(5) Environmental Benefit

The reduction rate of construction waste (I_{51}) measures the decrease in solid waste generation during construction relative to a baseline. Compared with traditional construction, which involves frequent on-site cutting, rework, and secondary processing, MEP prefabricated construction reduces waste at the source through precise factory cutting, standardized manufacturing, and BIM-based design checks and error prevention.

The Dust Compliance Rate (I_{52}) reflects the effectiveness of dust control during construction, represented by the proportion of monitoring results meeting standards. Prefabricated MEP construction reduces on-site cutting, grinding, and temporary modifications, effectively lowering dust emissions while enhancing site safety and environmental management. Previous studies generally suggest that prefabricated and off-site construction methods can reduce waste generation, air emissions, and environmental impacts compared with conventional construction.

2.3. Evaluation Model Construction

To systematically evaluate the comprehensive benefits of prefabricated electromechanical construction in energy station projects, this study develops an evaluation model based on a combination of subjective and objective weighting methods. Specifically, AHP

is employed to incorporate expert judgments from multiple domains and determine the structural weights of the indicator system. Meanwhile, the entropy method is applied to actual project data to capture the variability of indicators and derive objective weights. On this basis, the subjective and objective weights are integrated using a multiplicative normalization approach, which effectively balances expert knowledge with data-driven insights and improves the robustness and interpretability of the evaluation results.

2.3.1. Determination of Subjective Weights

This study determines subjective weights using a group AHP method. Expert elicitation was conducted with 50 project-related specialists from construction management organizations, design institutes, contractors, research institutions, and universities. The pairwise-comparison questionnaires were screened for completeness, internal consistency, and non-redundancy of judgment patterns. Because many responses showed highly similar and added limited information to the group judgment matrix, nine valid responses with clearer discriminatory information were retained for the group AHP aggregation. The retained experts had direct knowledge of the case project and relevant professional experience, supporting project-specific and technically grounded judgements.

Each expert performed pairwise comparisons of elements at the same level with respect to the upper-level objective based on the Saaty 1–9 scale, thereby forming individual judgment matrices [32].

Considering that this study involves group decision-making, the individual judgments are first aggregated before weight derivation. Let the judgment matrix provided by the k expert be $A^{(k)} = \left[a_{ij}^{(k)}\right]$, and the elements of the group judgment matrix are synthesized using the geometric mean method, as shown in Formula (3).

$$a_{ij} = \left(\prod_{k=1}^{K} a_{ij}^{(k)}\right)^{1/K} \tag{3}$$

where K denotes the number of experts, with $K = 9$ in this study. Based on this principle, the scoring scale derived from the group judgment matrix can be obtained. Table 2 presents the scoring scale between the objective layer and the criterion layer in group judgment matrix.

Table 2. Scoring scale between the objective layer and the criterion layer in the group judgment matrix.

G	C_1	C_2	C_3	C_4	C_5
C_1	1.0000	1.0293	1.8098	1.4546	2.4897
C_2	0.9716	1.0000	1.3264	1.4025	2.0038
C_3	0.5525	0.7539	1.0000	1.1958	1.4422
C_4	0.6875	0.7130	0.8363	1.0000	1.0086
C_5	0.4017	0.4991	0.6934	0.9915	1.0000

Since schedule benefit (C_1) and cost benefit (C_3) each contain only one secondary indicator, their local subjective weights are fixed at 1 and do not constitute local judgment matrices. Similarly, the scoring scales for the indicator layers of quality benefit (C_2) and safety benefit (C_4) in group judgment matrix can be obtained, as shown in Table 3. The scoring scale for the indicator layer of environmental benefit (C_5) in group judgment matrix is presented in Table 4.

Table 3. Scoring scales for the indicator layers of quality benefit and safety benefit in the group judgment matrix.

C_2	I_{21}	I_{22}	I_{23}	C_4	I_{41}	I_{42}	I_{43}
I_{21}	1.0000	0.8851	1.3639	I_{41}	1.0000	1.3511	2.2016
I_{22}	1.1298	1.0000	2.1409	I_{42}	0.7402	1.0000	2.3072
I_{23}	0.7332	0.4671	1.0000	I_{43}	0.4542	0.4334	1.0000

Table 4. Scoring scales for the indicator layers of environmental benefit in the group judgment matrix.

C_5	I_{51}	I_{52}
I_{51}	1.0000	3.0313
I_{52}	0.3299	1.0000

After obtaining the group judgment matrix, the local subjective weights of elements at each level are determined using the principal eigenvector method. Specifically, eigenvalue decomposition is performed on the group judgment matrix $A = (a_{ij})_{n\times n}$ to obtain the maximum eigenvalue $\lambda_{\max}$ and its corresponding eigenvector w, which satisfy the following equation:

$$A\omega = \lambda_{\max}\omega,\ \sum_{i=1}^{n} w_i = 1,\ w_i > 0 \tag{4}$$

To test the consistency of the judgment matrix, the consistency index (CI) and consistency ratio (CR) are introduced:

$$CI = \frac{\lambda_{\max} - n}{n-1},\ CR = \frac{CI}{RI} \tag{5}$$

When $CR < 0.10$, the judgment matrix is considered to have satisfactory consistency. It should be noted that when a level contains only a single criterion (e.g., C_1 and C_3), consistency testing is not required; when it is a second-order judgment matrix (e.g., C_5), because the random consistency index $RI = 0$, the conventional CR determination standard is also not applicable. The consistency test results of the group AHP judgment matrices are presented in Table 5.

Table 5. Consistency test results of the group AHP judgment matrices.

Judgment Matrix	Order (n)	λ_{max}	*CI*	*RI*	*CR*	Consistency Explanation
objective layer—criterion layer	5	5.0291	0.0073	1.12	0.0065	$CR < 0.1$
C_2	3	3.0120	0.0060	0.58	0.0104	$CR < 0.1$
C_4	3	3.0135	0.0067	0.58	0.0116	$CR < 0.1$

After the group judgment matrices pass the consistency test, the normalized principal eigenvector of the objective–criterion-level group judgment matrix is taken as the subjective weight of each criterion. Let w_c denote the subjective weight of criterion c, and $w_{j|c}$ denote the local subjective weight of indicator j under criterion c. Then, the global subjective weight of indicator j is given by:

$$W_j = w_c \cdot w_{j|c} \tag{6}$$

In Formula (6), W_j represents the global subjective contribution of indicator j to the overall objective. Based on the eigenvector results of the group judgment matrices that

passed the consistency test, the subjective weights at the criterion level, the local subjective weights, and the global subjective weights obtained for prefabricated MEP systems in energy stations are presented in Table 6.

Table 6. Subjective weights of the criterion layer based on AHP for prefabricated MEP systems in energy stations.

Criterion Layer	Subjective Weight of the Criterion Layer	Indicator Layer	Local Subjective Weight	Global Subjective Weight
C_1	0.2821	I_{11}	1.0000	0.2821
C_2	0.2476	I_{21}	0.3427	0.0849
		I_{22}	0.4321	0.1070
		I_{23}	0.2252	0.0558
C_3	0.1793	I_{31}	1.0000	0.1793
C_4	0.1616	I_{41}	0.4473	0.0723
		I_{42}	0.3718	0.0601
		I_{43}	0.1809	0.0292
C_5	0.1294	I_{51}	0.7519	0.0973
		I_{52}	0.2481	0.0321

According to the above table, under the group AHP framework, progress efficiency and quality benefit have relatively higher subjective weights at the criterion layer, followed by cost, safety, and environmental efficiency. At the indicator layer, I_{11}, I_{31}, I_{22}, and I_{51} exhibit relatively higher global subjective weights.

2.3.2. Determination of Objective Weights

After obtaining the subjective weights based on the AHP method, it is necessary to further introduce an objective weighting approach to refine the importance of each indicator from a data-driven perspective. The AHP method primarily relies on expert judgment, which effectively reflects the goal orientation of engineering management and the relative importance among indicators. However, as a subjective weighting approach, it is limited in its ability to capture the actual variability and informational differences among indicators across evaluation objects [33]. Therefore, it is essential to incorporate an objective method that reflects data characteristics to complement the AHP results.

In this study, the entropy method is adopted to objectively adjust the indicator weights. Based on the concept of information entropy, this method measures the degree of dispersion of indicator values to reflect the amount of information they contain: the greater the variability of an indicator, the more information it provides, the higher its weight. It should be noted that the entropy method is not intended to replace expert judgment derived from AHP but rather to serve as a complementary tool for data-driven correction, thereby enhancing the objectivity and robustness of the weighting results [30,34].

Regarding sample selection, four energy station construction units within the project are selected as samples for objective weighting, including two traditional construction samples (T_1 and T_2) and two prefabricated electromechanical construction samples (P1 and P2). These are denoted as $i = 1, 2, \ldots, m$, where $m = 4$. These four units were treated as comparable within-case observations rather than as a population-level sample. The resulting entropy weights capture project-specific indicator variation. For confidentiality reasons, only anonymized inputs and derived results are reported. A total of 10 evaluation indicators are considered, denoted as $j = 1, 2, \ldots, n$, where $n = 10$. First, based on the

quantification formulas for each indicator, the original project records are transformed into sample-level evaluation values, denoted uniformly as x_{ij}.

For indicator processing, to ensure consistency and rationality in the weighting procedure, the indicators are classified into two categories:

(1) State-type indicators, which directly reflect system performance or management outcomes (e.g., first-time acceptance pass rate), for which actual observed values are used.

(2) Comparative indicators, which reflect performance improvements through comparison (e.g., construction duration and cost). These indicators are normalized using the mean values of the traditional construction samples as benchmarks and transformed into benefit-type indicators.

The quantification methods and calculation criteria for each indicator are presented in Table 7. In this table, i denotes the number of the station-level construction unit, while T_0, r_0, C_0, E_0, f_0 and W_0 represent the mean values of the traditional construction sample group in terms of key construction duration, proportion of rework man-hours, total cost, high-risk operation exposure index, frequency of near-miss incidents, and construction waste generation, respectively.

Table 7. Quantification methods and calculation criteria for each indicator.

Indicator Layer	Sample-Level Quantification Formula	Definition
I_{11}	$I_{11}^{(i)} = \frac{T_0 - T_i}{T_0}$	Calculated based on the key construction duration; the shorter the duration, the higher the indicator value.
I_{21}	$I_{21}^{(i)} = \frac{Q_{pass}^{(i)}}{Q_{total}^{(i)}}$	Ratio of the number of items passing the first acceptance to the total number of acceptance items; the greater the number of items passing the first acceptance, the higher the indicator value.
I_{22}	$I_{22}^{(i)} = \frac{D_{pass}^{(i)}}{D_{total}^{(i)}}$	Ratio of the number of systems passing the first commissioning to the total number of systems; the greater the number of systems passing the first commissioning, the higher the indicator value.
I_{23}	$I_{23}^{(i)} = \frac{r_0 - r_i}{r_0}, ri = \frac{H_{re}^{(i)}}{H_{tot}^{(i)}}$	Calculated based on the proportion of rework man-hours; the lower the proportion of rework, the higher the indicator value.
I_{31}	$I_{31}^{(i)} = \frac{C_0 - C_i}{C_0}$	Calculated based on the total construction cost; the lower the cost, the higher the indicator value.
I_{41}	$I_{41}^{(i)} = \frac{E_0 - E_i}{E_0}$	Calculated based on the composite high-risk operation exposure index; the lower the exposure, the higher the indicator value.
I_{42}	$I_{42}^{(i)} = \frac{f_0 - f_i}{f_0}, f_i = \frac{M_i}{H_{work}^{(i)}}$	Calculated based on the frequency of near-miss incidents; the lower the frequency, the higher the indicator value.
I_{43}	$I_{43}^{(i)} = \frac{S_{close}^{(i)}}{S_{total}^{(i)}}$	Ratio of the number of hazards closed on schedule to the total number of hazards; the greater the number of hazards closed on schedule, the higher the indicator value.
I_{51}	$I_{51}^{(i)} = \frac{W_0 - W_i}{W_0}$	Calculated based on the amount of construction waste generated; the lower the waste generation, the higher the indicator value.
I_{52}	$I_{52}^{(i)} = \frac{A_{pass}^{(i)}}{A_{total}^{(i)}}$	Ratio of the number of days meeting dust control standards to the total monitoring days; the greater the number of compliant days, the higher the indicator value.

Thus, the objective weight evaluation matrix for the construction stage of the prefabricated electromechanical system of the energy station can be obtained, as shown below. This matrix serves as the fundamental input for the entropy weight method calculation.

$$X = \begin{bmatrix} x_{1,1} & x_{1,2} & \cdots & x_{1,10} \\ x_{2,1} & x_{2,2} & \cdots & x_{2,10} \\ \vdots & \vdots & \ddots & \vdots \\ x_{4,1} & x_{4,2} & \cdots & x_{4,10} \end{bmatrix} \tag{7}$$

To eliminate the impact of differences in the dimensions and scales of various indicators, the range normalization method is employed to standardize the evaluation matrix, as shown in Equation (8).

$$z_{ij} = \begin{cases} \frac{x_{ij} - \min x_{ij}}{\max x_{ij} - \min x_{ij}} & , \max x_{ij} \neq \min x_{ij} \\ 1 & , \max x_{ij} = \min x_{ij} \end{cases} \tag{8}$$

where z_{ij} denotes the normalized value of the indicator, and the above expression satisfies $1 \leq i \leq m$. Based on the normalization, the proportion of the j-th indicator in the i-th sample is further calculated, as shown in Equation (9).

$$p_{ij} = \frac{z_{ij}}{\sum_{i=1}^{m} z_{ij}} \tag{9}$$

The information entropy of the j-th indicator is obtained by Equation (10) as follows.

$$e_j = -\frac{1}{In\ m} \sum_{i=1}^{m} p_{ij} In\ p_{ij} \tag{10}$$

Meanwhile, the difference coefficient and the objective weight can be expressed as follows.

$$d_j = 1 - e_j, w_j^{(E)} = \frac{1 - e_j}{\sum_{j=1}^{n} (1 - e_j)} \tag{11}$$

where d_j denotes its difference coefficient, $w_j^{(E)}$ denotes the objective weight of the j-th basic evaluation indicator, and it satisfies $\sum_{j=1}^{n} w_j^{(E)} = 1$.

Following the above steps, the objective weights of the 10 indicators can be obtained based on the sample data of the energy station and the evaluation matrix in Equation (7), as shown in Table 8.

2.3.3. Determination of Combined Subjective–Objective Weights

To comprehensively reflect both expert judgment and the informational characteristics of sample data, this study adopts a multiplicative normalization method to determine the combined weights. These weights are based on the subjective weights obtained from the AHP method and the objective weights derived from the entropy method. Let the subjective weight of the j-th indicator be $w_j^{(A)}$, and the objective weight be $w_j^{(E)}$. The combined weight $w_j^{(C)}$ is calculated as follows:

$$w_j^{(C)} = \frac{w_j^{(A)} w_j^{(E)}}{\sum_{j=1}^{n} w_j^{(A)} w_j^{(E)}} \tag{12}$$

where n denotes the total number of indicators, with n = 10. This method preserves expert experience and judgment while incorporating the dispersion characteristics of sample data to objectively adjust the indicator weights, thereby yielding a comprehensive weighting result that balances subjective cognition and objective information.

Table 8. Results of Objective Weight Calculation Based on the Entropy Method.

Indicator Layer	Entropy of Information (e_j)	Coefficient of Variation (d_j)	Objective Weight ($w_j^{(E)}$)
I_{11}	0.619133	0.380867	0.1070
I_{21}	0.727320	0.272680	0.0766
I_{22}	0.787240	0.212760	0.0598
I_{23}	0.637092	0.362908	0.1020
I_{31}	0.616124	0.383876	0.1079
I_{41}	0.574542	0.425458	0.1196
I_{42}	0.608763	0.391237	0.1099
I_{43}	0.606243	0.393757	0.1106
I_{51}	0.690071	0.309929	0.0871
I_{52}	0.574716	0.425284	0.1195

Based on the subjective weights obtained using the group AHP geometric mean method and the objective weights calculated by the entropy method, the final combined weights of each indicator are further derived, as presented in Table 9.

Table 9. Comparison of Subjective Weights, Objective Weights, and Combined Weights.

Indicator Layer	Subjective Weights ($w_j^{(A)}$)	Objective Weight ($w_j^{(E)}$)	Combined Weights ($w_j^{(C)}$)
I_{11}	0.2821	0.1070	0.3052
I_{21}	0.0849	0.0766	0.0658
I_{22}	0.1070	0.0598	0.0647
I_{23}	0.0558	0.1020	0.0575
I_{31}	0.1793	0.1079	0.1955
I_{41}	0.0723	0.1196	0.0874
I_{42}	0.0601	0.1099	0.0668
I_{43}	0.0292	0.1106	0.0327
I_{51}	0.0973	0.0871	0.0857
I_{52}	0.0321	0.1195	0.0388

2.3.4. Construction of the Fuzzy Comprehensive Evaluation Model

After obtaining the combined subjective–objective weights, this study further evaluates the overall benefits of different construction methods. Since the evaluation of MEP construction performance involves multiple indicators, some of which are characterized by uncertainty and fuzziness, relying solely on limited weight results is insufficient to fully capture the comprehensive impact of each indicator on the overall performance. Therefore, this study introduces the fuzzy comprehensive evaluation method to address fuzzy boundaries and incomplete information in the evaluation process, enabling the effective integration of multi-indicator information and quantitative assessment [35]. Compared

with ranking-oriented MCDM methods, the fuzzy comprehensive evaluation method is more suitable for this study because it can not only compare construction alternatives but also classify their comprehensive benefits into interpretable "low–medium–high" levels through membership degrees.

Based on the evaluation index system established in the preceding sections, the evaluation factor set is constructed as follows:

$$U = \{I_{11}, I_{21}, I_{22}, I_{23}, I_{31}, I_{41}, I_{42}, I_{43}, I_{51}, I_{52}\} \tag{13}$$

where U represents the comprehensive benefit evaluation factor set. Meanwhile, the evaluation grade set is defined as follows:

$$V = \{v_1, v_2, v_3\} \tag{14}$$

where v_1, v_2, v_3 represent the three evaluation levels of low, medium, and high comprehensive benefit, respectively. This three-level set was used to avoid artificial granularity in a small within-case comparison and to preserve engineering interpretability. To ensure consistency of dimensionality across all indicators, normalization is performed according to the method described above. Let the original value of evaluation object p on indicator j be x_{pi}, and its normalized value be denoted as y_{pi}, where $y_{pi} \in [0, 1]$.

On this basis, a triangular membership function is employed to construct the membership degrees for the three grades of "low–medium–high." The breakpoints 0, 0.5, and 1 correspond to the lower bound, midpoint, and upper bound of the normalized benefit scale. For any normalized indicator value y_{pi}, the membership function corresponding to the "low" level is defined as follows:

$$\mu_1(y_{pj}) = \begin{cases} 1 - 2y_{pj}, & 0 \le y_{pj} \le 0.5 \\ 0, & 0.5 \le y_{pj} \le 1 \end{cases} \tag{15}$$

The membership function corresponding to the "medium" level is defined as follows:

$$\mu_2(y_{pj}) = \begin{cases} 2y_{pj}, & 0 \le y_{pj} \le 0.5 \\ 2(1 - y_{pj}), & 0.5 \le y_{pj} \le 1 \end{cases} \tag{16}$$

The membership function corresponding to the "high" level is defined as follows:

$$\mu_3(y_{pj}) = \begin{cases} 0, & 0 \le y_{pj} \le 0.5 \\ 2y_{pj} - 1, & 0.5 \le y_{pj} \le 1 \end{cases} \tag{17}$$

where $\mu_1(y_{pj})$, $\mu_2(y_{pj})$, and $\mu_3(y_{pj})$ represent the membership degrees of evaluation object p on indicator j corresponding to the "low," "medium," and "high" levels, respectively, and they satisfy the following condition:

$$\mu_1(y_{pj}) + \mu_2(y_{pj}) + \mu_3(y_{pj}) = 1 \tag{18}$$

Accordingly, the membership degrees of evaluation object p across all indicators can be aggregated into a fuzzy relation matrix, as follows:

$$R^{(p)} = \begin{bmatrix} r_{1,1} & r_{1,2} & r_{1,3} \\ r_{2,1} & r_{2,2} & r_{2,3} \\ \vdots & \vdots & \vdots \\ r_{10,1} & r_{10,2} & r_{10,3} \end{bmatrix} \tag{19}$$

where $R^{(p)}$ denotes the fuzzy relation matrix of evaluation object p, r_{jk} represents the membership degree of indicator I_j to the evaluation grade v_k, specifically defined as follows:

$$r_{j1} = \mu_1(y_{pj}), r_{j2} = \mu_2(y_{pj}), r_{j3} = \mu_3(y_{pj}) \tag{20}$$

Therefore, each row of the resulting fuzzy evaluation matrix $R^{(p)}$ corresponds to the membership degree distribution of one indicator across the three levels of "low–medium–high," and the sum of the elements in each row equals 1.

3. Case Analysis

3.1. Project Case Description

This study selects an energy station plant room of a large-scale data center in Wuhan as the case study. The energy station provides cooling capacity for the data center through chiller units [36]. According to the cooling load requirements, four high-voltage variable-frequency centrifugal chillers, each with a cooling capacity of 6680 kW, are installed to supply chilled water at 12 °C/18 °C.

The three-dimensional BIM model for the energy station plant room is shown in Figure 2. It comprises a total of 22 modules, including the constant pressure make-up pipe, cooling water make-up pipe, cold storage tank supply pipe, chemical dosing water supply pipe, softened water tank, constant pressure equipment, sand filter, chemical dosing device, air-conditioning chilled water return pipe, air-conditioning chilled water supply pipe, cold storage supply pipe, cold storage return pipe, cooling water pump, chilled water pump, air-conditioning cooling water supply pipe, air-conditioning cooling water return pipe, heat recovery supply pipe, heat recovery return pipe, cold storage tank discharge return pipe, chiller unit, plate heat exchanger, and open cooling tower. Functionally, the system can be divided into four subsystems: the water treatment system, cooling water system, chilled water system, and heat recovery system.

To facilitate comparative analysis, the project adopts a modular construction approach, dividing the entire energy station into four construction units with equal workloads. Among them, two units adopt traditional MEP installation methods, while the other two employ prefabricated MEP installation. The evaluation boundary is the energy station plant room and its four MEP construction units; whole-building structural works and other data-center systems are outside the scope. Compared with conventional MEP installation, the prefabricated MEP construction process of the energy station is centered on the BIM model, achieving deep integration of design informatization and construction industrialization. In this workflow, BIM serves as the information backbone for model coordination, clash detection, fabrication detailing, and construction sequencing. The workflow is illustrated in Figure 3.

Compared with conventional MEP installation, the prefabricated MEP construction process in the investigated energy station was fundamentally BIM-enabled. In this workflow, BIM was not used merely as a visualization tool but as the technical basis for digital design, multidisciplinary coordination, fabrication detailing, and construction sequencing. The prefabricated components were generated from BIM-based design outputs, transformed into shop drawings and fabrication information, produced off-site, and then assembled on-site according to the coordinated model. Therefore, in this study, prefabricated

MEP installation is understood as a BIM-enabled construction process rather than a process independent of BIM application.

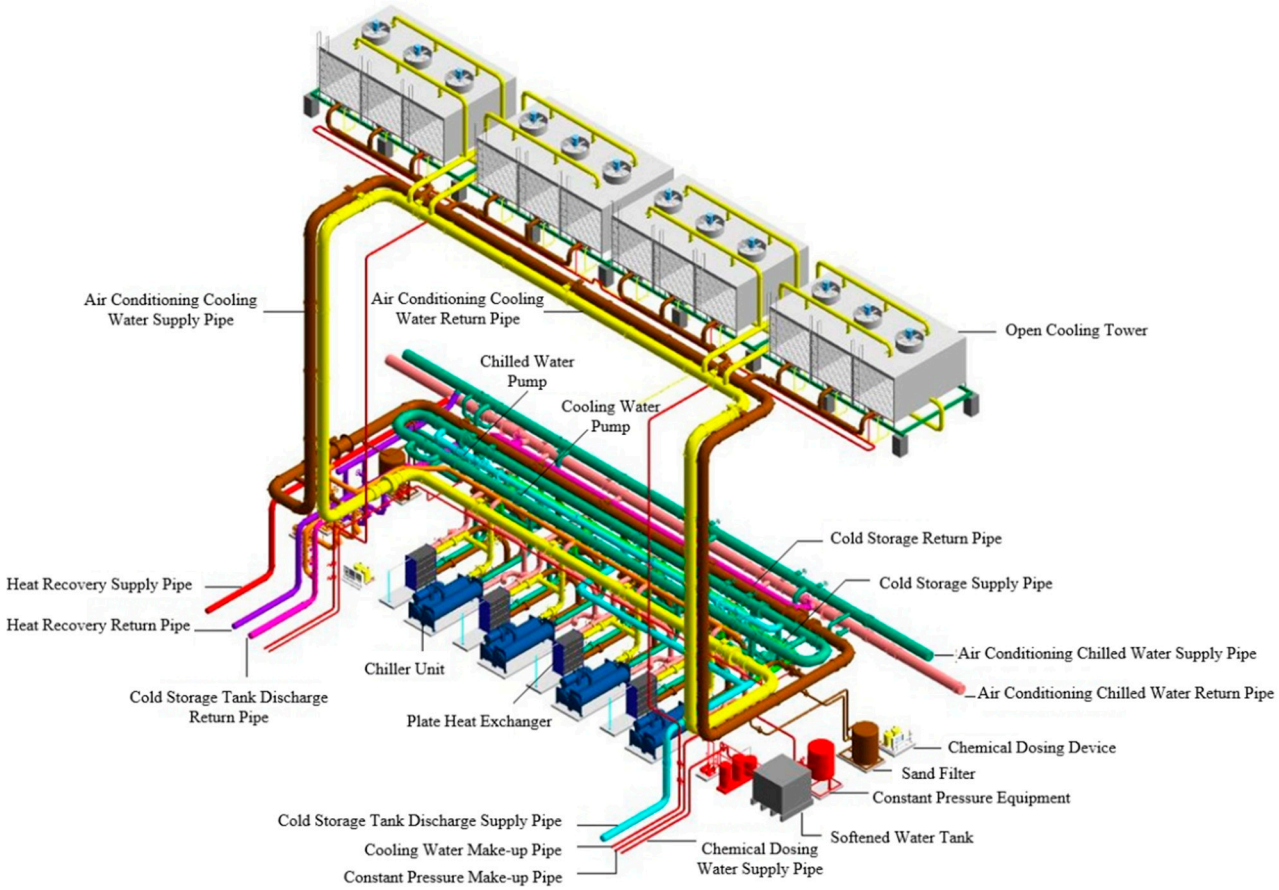


Figure 2. BIM model of the energy station plant room in this study.

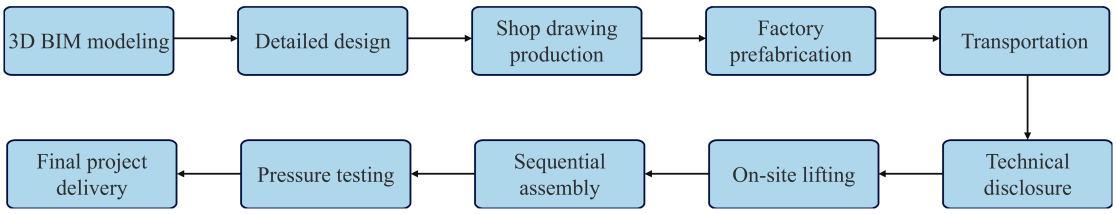


Figure 3. Workflow of the prefabricated MEP construction process of the energy station.

The process begins with 3D BIM modeling, where integrated architectural, structural, and MEP models are established using tools such as Revit 2024, incorporating both geometric and non-geometric information [37]. Based on this model, detailed design is conducted through platforms such as Navisworks to support multidisciplinary coordination, clash detection, pipeline optimization, and installation-interface checking. The model is then refined to Level of Development (LOD) 400 to support construction-level application. The refined BIM model is converted into shop drawings and fabrication information for standardized off-site prefabrication. Meanwhile, four-dimensional (4D) simulation is performed by integrating schedule information into the BIM model to optimize construction planning and installation sequencing [38]. During construction, prefabricated components are transported to the site and assembled according to the coordinated installation sequence. Finally, pressure testing, commissioning, and quality inspections are carried out to ensure system compliance before project delivery [39].

3.2. Project Ledger Data

This study conducts a statistical analysis of ten indicators across five dimensions—schedule, quality, safety, cost, and environmental performance—for the energy station plant room of a data center project in Wuhan, comparing the traditional MEP installation method with the prefabricated MEP construction approach. Based on the quantitative evaluation methods for each indicator presented in Table 7, the comparative results are summarized in Table 10.

Table 10. Comparison of Case Sample Ledger Summary and Quantitative Results for the Energy Station Plant Room Project.

Indicator Layer	Observation Item	Traditional MEP Installation Method	Prefabricated MEP Installation Method	Comparative Results
I_{11}	Construction duration	127.5 h	101.0 h	Decreased by 20.78%
I_{21}	Number of items passed the initial acceptance/Total number of acceptance items	113/122 (92.62%)	136/140 ((97.14%)	Increased by 4.88%
I_{22}	Number of systems successfully debugged on the first attempt/Total number of systems debugged	24/27 (88.89%)	33/35 (94.29%)	Increased by 6.07%
I_{23}	Rework hours/Total hours	80 h/1270 h (6.30%)	39 h/970 h (4.02%)	Decreased by 36.17%
I_{31}	Construction cost	¥842.3 × 10^4	¥858.6 × 10^4	Increased by 1.94%
I_{41}	Average High-Risk Work Exposure Index	35.95	31.65	Decreased by 11.96%
I_{42}	Number of near-miss incidents/Total hours	13/1270 h (0.010236)	6/970 h (0.006186)	Decreased by 39.57%
I_{43}	Number of hazards resolved on schedule/Total number of hazards	84/97 (86.60%)	92/98 (93.88%)	Increased by 8.41%
I_{51}	Total volume of construction waste	0.404 t	0.119 t	Reduced by 70.54%
I_{52}	Duration of dust emission compliance/Total monitoring duration	117 h/131 h (89.31%)	125 h/131 h (95.42%)	Increased by 6.84%

From the perspective of schedule and efficiency (I_{11}), the prefabricated construction method significantly optimizes the critical construction path. The key construction duration is reduced from 127.5 h to 101.0 h, representing a decrease of 20.78%, which indicates a clear advantage in construction organization and resource coordination. In terms of quality (I_{21}–I_{23}), the first-pass acceptance rate increases from 92.62% to 97.14%, and the first-time commissioning pass rate improves from 88.89% to 94.29%. Meanwhile, the proportion of rework hours decreases from 6.30% to 4.02%, with a reduction of 36.17%. These results demonstrate that prefabricated construction effectively enhances construction quality and reduces rework through standardized production and upfront verification. Regarding cost (I_{31}), the construction-phase cost shows a slight increase (+1.94%), reflecting a certain cost premium associated with upfront investment and industrialized production in pre-

fabricated construction; however, the overall increase remains within a controllable range. In terms of safety (I_{41}–I_{43}), the prefabricated approach exhibits significant advantages: the high-risk operation exposure index decreases by 11.96%, the near-miss incident rate declines by 39.57%, and the hazard closure rate increases by 8.41%. This indicates that reducing on-site high-risk operations and improving management refinement effectively enhance construction safety performance. From the environmental perspective (I_{51}–I_{52}), the total construction waste is significantly reduced from 0.404 t to 0.119 t (a decrease of 70.54%), and the dust compliance rate increases from 89.31% to 95.42%, demonstrating notable advantages of prefabricated construction in green construction and environmental performance.

Overall, except for a slight increase in direct construction cost, the BIM-enabled prefabricated MEP construction method outperforms the traditional construction approach across multiple key dimensions, including schedule, quality, safety, and environmental performance. This indicates a strong comprehensive benefit advantage within the scope of the case study.

4. Results and Discussion

4.1. Evaluation Analysis

After obtaining the combined weights, this study further employed the fuzzy comprehensive evaluation method to assess the overall benefits of the conventional MEP construction method and the prefabricated MEP construction method. Based on the fuzzy comprehensive evaluation model established in Section 2.3.4, the records of the two traditional units and the two prefabricated units were first aggregated at the scheme level. The resulting scheme-level values were then positively normalized using the indicator directions and normalization ranges derived from the unit-level evaluation matrix used in the entropy-weighting procedure. The standardized scheme-level input vectors are presented in Table 11.

Table 11. Standardized scheme-level input vectors.

Construction Method	I_{11}	I_{21}	I_{22}	I_{23}	I_{31}	I_{41}	I_{42}	I_{43}	I_{51}	I_{52}
Traditional MEP installation method	0.051724	0.172131	0.363636	0.063172	0.727642	0.028302	0.080645	0.041865	0.116564	0.031677
Prefabricated MEP installation method	0.965517	0.985714	0.981818	0.928441	0.065041	0.839623	0.678283	0.984150	0.990798	0.803995

As shown in Table 11, all indicators satisfy the unidirectional requirement that "a larger value indicates better comprehensive performance." Among them, the traditional MEP construction method exhibits a relatively higher standardized value for indicator I_{31} (total cost variation rate), whereas the prefabricated MEP construction method demonstrates higher standardized results across most indicators related to schedule, quality, safety, and environmental performance. This indicates that, within the scope of the case study, although the prefabricated MEP construction method did not achieve a direct cost advantage, it showed significant improvements in multiple non-cost performance indicators. Accordingly, the prefabricated alternative should be interpreted as a multi-objective performance-improvement strategy with a limited cost premium rather than as a cost-minimization strategy.

On this basis, according to the triangular membership functions defined in Section 2.3.4, the standardized results of each indicator were mapped into a three-level linguistic assessment space of "low–medium–high," and the corresponding fuzzy relation matrices were constructed. The fuzzy relation matrices for the traditional MEP construction method and

the prefabricated MEP construction method are denoted as $R^{(T)}$ and $R^{(B)}$, respectively. Each row of the matrix represents the membership degree distribution of a given indicator across the three evaluation levels ("low," "medium," and "high"), with the sum of membership degrees equal to 1.

The comprehensive weighting vector is taken from the subjective–objective combined weights reported in Table 9, namely:

$$U = (0.3052, 0.0658, 0.0647, 0.0575, 0.1955, 0.0874, 0.0668, 0.0327, 0.0857, 0.0388) \quad (21)$$

where each component corresponds respectively to the combined weights of indicators I_{11} to I_{52}. It can be observed that I_{11} (schedule improvement rate) and I_{31} (total cost variation rate) are assigned relatively higher weights, indicating that schedule performance and cost constraints are the key factors influencing the overall evaluation results.

By substituting the fuzzy relation matrix $R^{(T)}$ of the traditional construction method into the model, its comprehensive evaluation vector is obtained as:

$$B^{(T)} = U \cdot R^{(T)} = (0.655073, 0.255906, 0.089021) \quad (22)$$

The results indicate that the traditional construction method has the highest membership degree in the "low" category, reaching 0.6551, while the membership degree in the "high" category is only 0.0890. According to the principle of maximum membership degree, the comprehensive evaluation level of the traditional construction method can be classified as "low." This result suggests that, under the conditions of the present case study, the traditional construction method lacks sufficient support in terms of schedule performance, safety, rework control, and environmental performance, and its overall comprehensive benefits are relatively weak.

Similarly, by substituting the fuzzy relation matrix $R^{(B)}$ of the prefabricated MEP construction method into the model, the following result is obtained:

$$B^{(B)} = U \cdot R^{(B)} = (0.170093, 0.147770, 0.682137) \quad (23)$$

The results show that the prefabricated MEP construction method has the highest membership degree in the "high" category, reaching 0.6821, which is significantly higher than those of the "low" and "medium" categories. Therefore, according to the principle of maximum membership degree, its comprehensive evaluation level is classified as "high." This result indicates that the prefabricated MEP construction method demonstrates a clear overall advantage under the integrated multi-indicator evaluation framework.

To further enhance comparability between the two construction methods, this study quantifies the evaluation set according to Section 2.3.4 as:

$$V = (50, 75, 100) \quad (24)$$

where the three linguistic grades "Low", "Medium", and "High" are assigned values of 50, 75, and 100, respectively. These values provide an ordinal-to-numeric mapping for comparative scoring rather than absolute performance thresholds. Accordingly, the comprehensive score of each evaluation object can be expressed as:

$$F_p = B^{(p)} V^{\mathbf{T}} \quad (25)$$

Based on this, the comprehensive score of the traditional construction method is:

$$F_T = B^{(T)} V^{\mathbf{T}} = 0.655073 \times 50 + 0.255906 \times 75 + 0.089021 \times 100 = 60.85 \quad (26)$$

The comprehensive score of the prefabricated MEP construction method is:

$$F_B = B^{(B)} V^{\mathbf{T}} = 0.170093 \times 50 + 0.147770 \times 75 + 0.682137 \times 100 = 87.80 \quad (27)$$

The final fuzzy comprehensive evaluation results for the two construction methods are presented in Table 12.

Table 12. Fuzzy Comprehensive Evaluation Results of the Traditional MEP Construction Method and the Prefabricated MEP Construction Method.

Construction Method	B1 (Low)	B2 (Medium)	B3 (High)	Overall Score (F)	Judgment Level
Traditional MEP installation method	0.6551	0.2559	0.0890	60.85	low
Prefabricated MEP installation method	0.1701	0.1478	0.6821	87.80	high

The fuzzy comprehensive evaluation results show that, at the unit-level construction element of the same energy station, the prefabricated MEP construction method achieves a higher comprehensive score (87.80) than the traditional method (60.85). The prefabricated method has a dominant membership in the "high" category, while the traditional method is mainly concentrated in the "low" category. This confirms that the AHP–Entropy–Fuzzy model can effectively differentiate the overall performance levels of the two construction methods.

4.2. TOPSIS-Based Sensitivity Analysis

To assess the sensitivity of the ranking results to changes in criterion weights, TOPSIS was applied as a supplementary analysis [40,41]. This analysis was used only to examine the ranking stability of the four comparable units within the same project, rather than to make population-level statistical inference. The TOPSIS closeness coefficients were used solely for sensitivity testing and were not combined with the fuzzy comprehensive evaluation scores.

The final combined weights were used as the baseline scheme. For each scenario s, one first-level criterion group was perturbed by 10%, 20% or 50%, while the other indicators were unchanged before renormalization. The TOPSIS procedure was defined as:

$$\begin{cases} w_j^{(s)} = [w_j(1+\delta_j^{(s)})] / \sum_{j=1}^{10} w_j(1+\delta_j^{(s)}) \\ C_i^{(s)} = \dfrac{D_i^{-(s)}}{D_i^{+(s)} + D_i^{-(s)}} \\ \Delta\overline{C}^{(s)} = \overline{C}_{pref}^{(s)} - \overline{C}_{conv}^{(s)} \end{cases} \quad (28)$$

Here, w_j is the baseline combined weight of indicator j, $w_j^{(s)}$ is the renormalized weight in scenario s, and $\delta_j^{(s)}$ is the perturbation coefficient. For indicators in the perturbed criterion group, $\delta_j^{(s)} = \pm 0.10$, ± 0.20, or ± 0.50, otherwise, $\delta_j^{(s)} = 0$. $C_i^{(s)}$ is the TOPSIS closeness coefficient of sample i, and $D_i^{+(s)}$ and $D_i^{-(s)}$ are its Euclidean distances from the positive and negative ideal solutions, respectively. $\overline{C}_{conv}^{(s)}$ is the mean closeness coefficient of T-1 and T-2, while $\overline{C}_{pref}^{(s)}$ is the mean closeness coefficient of P-1 and P-2. A positive $\Delta\overline{C}^{(s)}$ indicates that the BIM-enabled prefabricated group remains closer to the positive ideal solution.

As shown in Table 13, all $\Delta\overline{C}^{(s)}$ values remained positive across the tested perturbation levels. The conventional group had mean closeness coefficients between 0.2068 and 0.3863, whereas the BIM-enabled prefabricated group ranged from 0.5464 to 0.7721. The smallest gap was observed when the progress weight was reduced by 50% ($\Delta\overline{C}^{(s)} = 0.1601$). Under the 50% cost-increase scenario, the BIM-enabled prefabricated group also retained a higher mean closeness coefficient than the conventional group, with values of 0.5517 and 0.3768, respectively.

Table 13. TOPSIS-based sensitivity analysis under criterion-weight perturbations.

Perturbation Level	Criterion Group	$\overline{C}_{conv}(+)$	$\overline{C}_{pref}(+)$	$\Delta\overline{C}(+)$	$\overline{C}_{conv}(-)$	$\overline{C}_{pref}(-)$	$\Delta\overline{C}(-)$
Baseline	Combined weights	0.3031	0.6450	0.3419	—	—	—
10%	C1 Progress	0.2892	0.6614	0.3722	0.3181	0.6274	0.3093
10%	C2 Quality	0.3039	0.6473	0.3434	0.3025	0.6430	0.3405
10%	C3 Cost	0.3196	0.6240	0.3044	0.2857	0.6674	0.3817
10%	C4 Safety	0.3010	0.6460	0.3450	0.3052	0.6441	0.3390
10%	C5 Environment	0.3020	0.6467	0.3447	0.3042	0.6435	0.3393
20%	C1 Progress	0.2764	0.6766	0.4003	0.3341	0.6085	0.2744
20%	C2 Quality	0.3045	0.6497	0.3452	0.3018	0.6411	0.3393
20%	C3 Cost	0.3352	0.6043	0.2691	0.2674	0.6913	0.4240
20%	C4 Safety	0.2987	0.6471	0.3484	0.3070	0.6433	0.3363
20%	C5 Environment	0.3007	0.6484	0.3477	0.3052	0.6422	0.3370
50%	C1 Progress	0.2432	0.7158	0.4726	0.3863	0.5464	0.1601
50%	C2 Quality	0.3065	0.6577	0.3513	0.3000	0.6365	0.3366
50%	C3 Cost	0.3768	0.5517	0.1749	0.2068	0.7721	0.5653
50%	C4 Safety	0.2910	0.6505	0.3595	0.3114	0.6414	0.3300
50%	C5 Environment	0.2965	0.6543	0.3578	0.3075	0.6390	0.3315

These results indicate that the comparative ranking was stable under substantial criterion-weight variation. Within the project-level comparison, the BIM-enabled prefabricated MEP method remained consistently closer to the positive ideal solution than the conventional method, supporting the robustness of the main evaluation results.

After assessing the stability of the evaluation outcome, the baseline weighting structure was further examined. A heatmap of the AHP, entropy, and combined weights was constructed to identify the dominant indicators in the original evaluation model, as shown in Figure 4, which is constructed to visualize the distribution characteristics of weights under different weighting approaches and the overall influence structure of the evaluation indicators.

Figure 4 traces the baseline weight structure behind the stable classification reported in Table 13. The following analysis identifies the indicators with the greatest leverage in the original evaluation model.

First, from the perspective of subjective weights (AHP), indicators such as I_{11} (schedule improvement rate), I_{31} (total cost variation rate), I_{22} (first-pass commissioning rate), and I_{51} (construction waste reduction rate) are assigned relatively higher weights, indicating that experts place greater emphasis on traditional management objectives such as schedule, cost, and project delivery quality. Among them, I_{11} reaches 0.2821, making it the most important subjective indicator.

Second, from the perspective of objective weights (Entropy), I_{41} (reduction in high-risk operation exposure index), I_{42} (reduction in near-miss event frequency), I_{43} (timely closure rate of safety hazards), and I_{52} (dust emission compliance rate) receive higher weights,

suggesting that these indicators exhibit stronger variability and discriminative power in the sample data and better capture differences between construction methods.

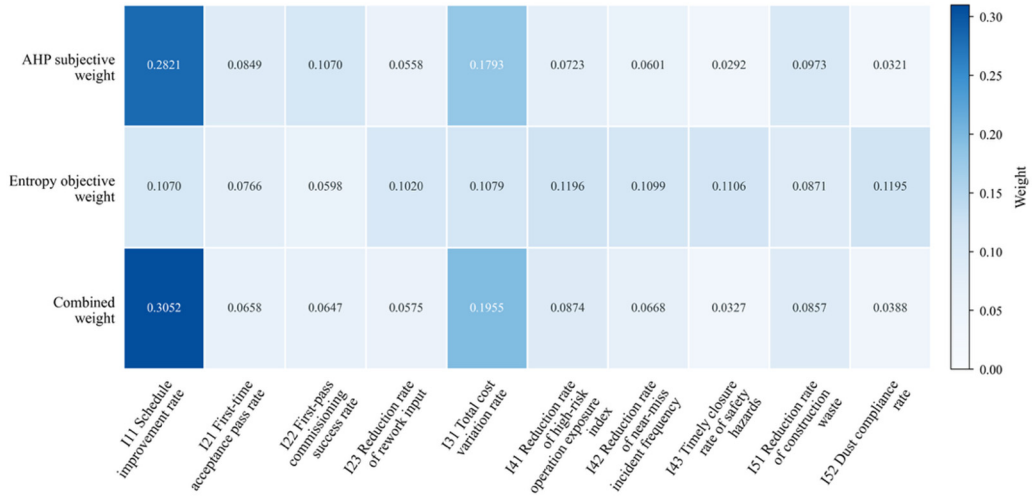


Figure 4. Heatmap of indicator weights based on the AHP–Entropy combined weighting method.

At the level of combined weights, I_{11} (0.3052) and I_{31} (0.1955) emerge as the two dominant drivers, forming a "dual-core" structure of the comprehensive evaluation. Meanwhile, I_{41} (0.0874) and I_{51} (0.0857) provide important supporting roles in the safety and environmental dimensions. This structure indicates that the overall evaluation is primarily driven by "schedule benefits and cost constraints," complemented by improvements in safety and environmental performance.

Further comparison shows that some indicators with relatively large improvement magnitudes contribute marginally to the final evaluation due to their low combined weights, such as I_{42} and I_{23}. In contrast, although I_{31} reflects a cost increase (1.94%), its high weighting makes it a critical constraint factor in the final assessment. This demonstrates that the evaluation outcome is not determined solely by the magnitude of performance improvement, but by the joint effect of the weight structure and directional performance.

From the perspective of fuzzy comprehensive evaluation interpretation, the reason why the prefabricated MEP construction method is classified as "high" is not because all indicators are superior, but because high-weight indicators (I_{11}, I_{31}) and key supporting indicators (I_{41}, I_{51}) simultaneously exhibit favorable or acceptable performance, leading to an aggregated advantage effect through fuzzy synthesis (0.6821). In contrast, the traditional construction method is mainly concentrated in the "low" category (0.6551) due to weaker performance in key high-weight indicators.

Overall, Figure 4 reveals a key finding: the comprehensive evaluation results are fundamentally driven by a "schedule–cost dual-core structure," while safety and environmental indicators provide supplementary constraints and explanatory reinforcement. In the context of energy station systems characterized by strong MEP coupling, the advantages of the prefabricated MEP construction method are primarily reflected in improved system-level organizational efficiency and proactive risk control, rather than pure cost optimization. Therefore, it is more appropriately characterized as a "multi-objective integrated optimization construction mode" rather than the cost-optimized solution alone.

These findings clarify the practical value of BIM-enabled prefabricated MEP construction in the investigated energy station plant room. For project owners, the results indicate that prefabricated MEP delivery can improve overall construction performance under a limited construction stage cost premium. For contractors, it suggests that transferring part of the work to controlled off-site fabrication can reduce site uncertainty and construction

variability. For designers and supervisors, the BIM-based prefabrication process provides a traceable basis for coordination, fabrication control, and performance verification. Although these findings remain case-specific, the results show that the AHP–Entropy–Fuzzy evaluation model can link technical performance with managerial decision-making under cost constraints.

5. Conclusions

In the investigated energy station plant room case, BIM-enabled prefabrication achieved higher overall performance than conventional MEP installation. This advantage was not attributable to lower direct costs. Instead, faster delivery and improved construction-process outcomes offset a limited construction stage cost premium.

The AHP–Entropy–Fuzzy framework provides a transparent route for converting heterogeneous ledger records into comparable benefit levels. It integrates expert judgment, project data variation, and fuzzy membership to support project-level interpretation under uncertainty.

The prefabricated method achieved a score of 87.80 and was classified as "high", whereas the conventional method scored 60.85 and was classified as "low". The TOPSIS-based sensitivity analysis further showed that, under 10%, 20%, and 50% criterion-weight perturbation scenarios, the prefabricated group consistently achieved higher TOPSIS closeness coefficients than the conventional group. The mean closeness coefficient ranged from 0.5464 to 0.7721 for the prefabricated group and from 0.2068 to 0.3863 for the conventional group. The smallest difference occurred when the schedule weight was reduced by 50%. Even under this condition, the prefabricated group retained a positive advantage $(\Delta\overline{C} = 0.1601)$, indicating that the ranking remained stable across a broad range of criterion-weight variations. Therefore, the prefabricated method should be interpreted as a case-specific performance optimization strategy rather than a cost-minimization solution.

This study is limited to a single energy station plant room case. Because the four construction units are within-case observations, the entropy weights and fuzzy scores should be interpreted as project-specific estimates rather than population-level statistical results. In addition, the cost metric used in this study covers only direct construction stage expenditure. Broader life-cycle costs, such as design coordination, factory production, transportation, long-term maintenance, operational impacts, downtime, and carbon-related costs, were outside the available data boundary. Future research should test the framework across multiple projects and incorporate life-cycle cost and carbon assessments once post-construction and operational data become available.

Author Contributions: Conceptualization, S.G., M.A.K. and J.Z.; Methodology, Y.L. (Yuxuan Liu), Y.L. (YungHao Loh) and J.Z.; Software, Y.L. (Yuxuan Liu) and Y.L. (YungHao Loh); Validation, Y.L. (YungHao Loh); Formal analysis, M.A.K.; Resources, F.Z.; Data curation, Y.L. (Yuxuan Liu); Writing—original draft, Y.L. (Yuxuan Liu); Writing—review and editing, Y.L. (Yuxuan Liu) and J.Z.; Supervision, S.G., M.A.K. and J.Z.; Project administration, F.Z., M.A.K. and J.Z.; Funding acquisition, F.Z., S.G., M.A.K. and J.Z. All authors have read and agreed to the published version of the manuscript.

Funding: This research was funded by Wuhan Key R&D Plan grant number [2023020402010590], Major R&D projects of China Metallurgical group corporation grant number [2022 No. 14], The PhD Scientific Research and Innovation Foundation of Sanya Yazhou Bay Science and Technology City grant number [HSPHDSRF-2022-03-002], the Project of Sanya Yazhou Bay Science and Technology City, grant number [SKJC-2022-PTDX-021] and the Environmental Health and Smart City Innovation Team, Project No. [KYTDP202503].

Institutional Review Board Statement: Ethical review and approval were waived for this study because the questionnaire only involved anonymized expert judgments for engineering indicator weighting, without collecting identifiable or sensitive personal data.

Informed Consent Statement: Informed consent for participation was obtained from all subjects involved in the study.

Data Availability Statement: The data presented in this study are available on request from the corresponding author.

Conflicts of Interest: Author Fan Zhang was employed by the company Wuhan Hengtai Hongan Safety Technology Co., Ltd. The remaining authors declare that the research was conducted in the absence of any commercial or financial relationships that could be construed as potential conflicts of interest.

References

1. Lv, G.; Cao, B.; Jun, L.; Liu, G.; Ding, Y.; Yu, J.; Zhang, Y.; Zhang, D. Optimal scheduling of integrated energy system under the background of carbon neutrality. *Energy Rep.* **2022**, *8*, 1236–1248. [CrossRef]
2. Rezaie, B.; Rosen, M.A. District heating and cooling: Review of technology and potential enhancements. *Appl. Energy* **2012**, *93*, 2–10. [CrossRef]
3. Zhou, Y.; Zheng, S.; Hensen, J.L.M. Machine learning-based digital district heating/cooling with renewable integrations and advanced low-carbon transition. *Renew. Sustain. Energy Rev.* **2024**, *199*, 114466.
4. Zhang, J.; Wang, Q.; Gui, S.; Zhou, J.; Sun, J. Identification of the key issues and technical paths for intelligent operation of water source heat pump energy stations applying digital twin technology. *Appl. Sci.* **2024**, *14*, 5094. [CrossRef]
5. Zhang, J.; Sun, J.; Zhao, H.; Huang, F.; Xu, B.; Wang, Q. Toward Smart and Green Energy Stations: A Cognitive Digital Twin Framework for Intelligent Management. *IEEE Internet Comput.* **2026**, *30*, 46–55. [CrossRef]
6. Du, J.; Zhang, J.; Castro-Lacouture, D.; Hu, Y. Lean manufacturing applications in prefabricated construction projects. *Autom. Constr.* **2023**, *150*, 104790. [CrossRef]
7. Qi, B.; Razkenari, M.; Costin, A.; Kibert, C.; Fu, M. A systematic review of emerging technologies in industrialized construction. *J. Build. Eng.* **2021**, *39*, 102265. [CrossRef]
8. Zhang, Y.; Ma, J.; Zhang, X.; Feng, S.; Fu, E.; Cheng, J. Application of BIM Technology in Complex Energy Station Buildings. *J. Inf. Technol. Civ. Eng. Archit.* **2021**, *13*, 113–120.
9. Zhang, N.; Pan, J.; Wang, J. Typical Application and Specialized Technology of Modular Prefabricated Assembly Construction in Building Mechanical and Electrical Engineering. *Build. Constr.* **2022**, *44*, 584–587.
10. Guo, J.; Li, B.; Jing, H.; Hu, C.; Lin, S. Study on the impact of optimal design of internal space layout of pre-assembled substation on the stability of equipment operation. *Appl. Math.* **2025**, *10*, 1–16. [CrossRef]
11. Lavikka, R.; Chauhan, K.; Peltokorpi, A.; Seppänen, O. Value creation and capture in systemic innovation implementation: Case of mechanical, electrical and plumbing prefabrication in the Finnish construction sector. *Constr. Innov.* **2021**, *21*, 837–856. [CrossRef]
12. Valkonen, T.; Lindberg, A.; Alhava, O.; Talebi, S.; Koskela, L.; Seppänen, O. Tolerance management in prefabrication of mechanical, electrical, and plumbing installations. *Constr. Manag. Econ.* **2026**, *44*, 279–299. [CrossRef]
13. Cheng, B.; Huang, J.; Lu, K.; Li, J.; Gao, G.; Wang, T.; Chen, H. BIM-enabled life cycle assessment of concrete formwork waste reduction through prefabrication. *Sustain. Energy Technol. Assess.* **2022**, *53*, 102449. [CrossRef]
14. Gallo, P.; Romano, R.; Belardi, E. Smart green prefabrication: Sustainability performances of industrialized building technologies. *Sustainability* **2021**, *13*, 4701. [CrossRef]
15. Ding, Y.; Guo, Z.Z.; Zhou, S.X.; Wei, Y.Q.; She, A.M.; Dong, J.L. Research on carbon emissions during the construction process of prefabricated buildings based on BIM and LCA. *J. Asian Archit. Build. Eng.* **2025**, *24*, 1426–1438.
16. Tian, Y.; Spatari, S. Environmental life cycle evaluation of prefabricated residential construction in China. *J. Build. Eng.* **2022**, *57*, 104776. [CrossRef]
17. Zhai, Y.; Sun, Y.; Li, Y.; Tang, S. Design for Assembly (DFA) evaluation method for prefabricated buildings. *Buildings* **2023**, *13*, 2692. [CrossRef]
18. Liu, Y.; Zhang, B.; Qin, J.; Zhu, Q.; Lyu, S. Integrated Performance Assessment of Prefabricated Component Suppliers Based on a Hybrid Method Using Analytic Hierarchy Process–Entropy Weight and Cloud Model. *Buildings* **2024**, *14*, 3872. [CrossRef]
19. Xia, M.; Zhao, L.; Zhao, L. A comprehensive risk-assessment method for prefabricated buildings using EPC: A case study from China. *Sustainability* **2022**, *14*, 1910. [CrossRef]
20. Solapure, D.M.; Vyas, G.S.; Dalvi, R.S.; Nikhar, C.K. Integration of BIM-LCC for evaluation of sustainable construction methods using AHP and entropy. *Innov. Infrastruct. Solut.* **2025**, *10*, 520. [CrossRef]
21. Jato-Espino, D.; Castillo-Lopez, E.; Rodriguez-Hernandez, J.; Canteras-Jordana, J.C. A review of application of multi-criteria decision making methods in construction. *Autom. Constr.* **2014**, *45*, 151–162. [CrossRef]

22. Tan, T.; Mills, G.; Papadonikolaki, E.; Liu, Z. Combining multi-criteria decision making methods with building information modelling: A review. *Autom. Constr.* **2021**, *121*, 103451.
23. Wu, X.; Han, J.; Cui, H.; Li, T.; Bai, X.; He, Y.; Liu, N. A comparative review of recent research progress in prefabricated buildings in China and other countries. *Buildings* **2024**, *14*, 1062. [CrossRef]
24. Shahpari, M.; Saradj, F.M.; Pishvaee, M.S.; Piri, S. Assessing the productivity of prefabricated and in-situ construction systems using hybrid multi-criteria decision making method. *J. Build. Eng.* **2020**, *27*, 100979.
25. Abanda, F.H.; Tah, J.H.M.; Cheung, F.K.T. BIM in off-site manufacturing for buildings. *J. Build. Eng.* **2017**, *14*, 89–102. [CrossRef]
26. Zhang, Y.; Zhang, L.; Zhao, W.; Wei, C. Current status and future prospects of prefabricated buildings. *Acad. J. Archit. Geotech. Eng.* **2025**, *7*, 25–30. [CrossRef]
27. Daly, M.; Kempton, L.; McCarthy, T. Sustainability of prefabricated construction in Australia: Industry perspectives on challenges and opportunities. *J. Build. Eng.* **2025**, *102*, 111805. [CrossRef]
28. Sethy, B.P.; Gupta, P.; Chandra, A.; Sethi, K.C.; Behera, A.P.; Sharma, K. Optimizing construction time, cost, and quality: A hybrid AHP-NSGA-III model for enhanced multi-objective decision making. *Asian J. Civ. Eng.* **2025**, *26*, 1043–1057.
29. Hatefi, S.M.; Ahmadi, H.; Tamošaitienė, J. Risk assessment in mass housing projects using the integrated method of Fuzzy Shannon Entropy and fuzzy EDAS. *Sustainability* **2025**, *17*, 528. [CrossRef]
30. Ren, Q.; Sun, M. Using AHP-Entropy method to explore the influencing factors of spatial demand of EVs public charging stations: A case study of Jinan, China. *J. Clean. Prod.* **2025**, *491*, 144779. [CrossRef]
31. Zhao, X.; Yang, Q.; Fan, X.; Yan, G.; Liu, L.; Yang, Y.; Zhang, H. Review of module division methods for mechanical, electrical, and plumbing systems in construction. *J. Build. Eng.* **2025**, *101*, 111753. [CrossRef]
32. Salomon, V.A.P.; Gomes, L.F.A.M. Consistency Improvement in the Analytic Hierarchy Process. *Mathematics* **2024**, *12*, 828. [CrossRef]
33. Chai, N.; Zhou, W.; Hu, X. Safety evaluation of urban rail transit operation considering uncertainty and risk preference: A case study in China. *Transp. Policy* **2022**, *125*, 267–288. [CrossRef]
34. Li, X.; Peng, Y.; Guo, Y.; Wang, W.; Song, X. An integrated simulation and AHP-entropy-based NR-TOPSIS method for automated container terminal layout planning. *Expert Syst. Appl.* **2023**, *225*, 120197.
35. Yang, M.; Ji, Z.; Zhang, L.; Zhang, A.; Xia, Y. A hybrid comprehensive performance evaluation approach of cutter holder for tunnel boring machine. *Adv. Eng. Inform.* **2022**, *52*, 101546. [CrossRef]
36. Neri, M.; Guelpa, E.; Khor, J.O.; Romagnoli, A.; Verda, V. Hierarchical model for design and operation optimization of district cooling networks. *Appl. Energy* **2024**, *371*, 123667. [CrossRef]
37. Chong, O.W.; Zhang, J. Logic representation and reasoning for automated BIM analysis to support automation in offsite construction. *Autom. Constr.* **2021**, *129*, 103756. [CrossRef]
38. Huang, L.; Pradhan, R.; Dutta, S.; Cai, Y. BIM4D-based scheduling for assembling and lifting in precast-enabled construction. *Autom. Constr.* **2022**, *133*, 103999.
39. Jiang, Y.; Li, M.; Guo, D.; Wu, W.; Zhong, R.Y.; Huang, G.Q. Digital twin-enabled smart modular integrated construction system for on-site assembly. *Comput. Ind.* **2022**, *136*, 103594.
40. Bánhidi, Z.; Dobos, I. Sensitivity of TOPSIS ranks to data normalization and objective weights on the example of digital development. *Cent. Eur. J. Oper. Res.* **2024**, *32*, 29–44.
41. Gaona, À.; Guisasola, A.; Baeza, J.A. An integrated TOPSIS framework with full-range weight sensitivity analysis for robust decision analysis. *Decis. Anal. J.* **2025**, *17*, 100642. [CrossRef]

Disclaimer/Publisher's Note: The statements, opinions and data contained in all publications are solely those of the individual author(s) and contributor(s) and not of MDPI and/or the editor(s). MDPI and/or the editor(s) disclaim responsibility for any injury to people or property resulting from any ideas, methods, instructions or products referred to in the content.